2D BEAM STEERING USING ELECTROSTATIC AND THERMAL ACTUATION FOR NETWORKED CONTROL

Jitendra Makwana[1], Stephen Phillips[1], Lifeng Wang[1], Nathan Wedge[2], and Vincenzo Liberatore[2]
[1]Department of Electrical Engineering, Arizona State University
Tempe, AZ 85287-5706, USA
[2]Department of Electrical Engineering and Computer Science, Case Western Reserve University
10900 Euclid Avenue, Cleveland, OH 44106, USA

ABSTRACT

This paper presents a design for a two-dimensional electrostatic mirror for beam steering and introduces the concept of networked control systems. The design requirements are a maximum tilt angle of 5° and minimum power consumption. Theoretical models in electrostatic fields and mechanical fields are presented, which provide insights into the influences of the design parameters on performance. Coventor software is utilized in the design and analysis of the 2D beam steering using zipper electrostatic actuator. An additional thermal actuator is also designed, and results are presented. An overview of the networked control systems field is given along with potential applications of the actuator.

Keywords: cantilever beam, electrostatic, zipper actuator, thermal actuator, MEMS, networked control systems

I. INTRODUCTION

The development of more sophisticated MEMS actuator implementations creates potential for improved functionality in the increasingly significant field of networked control systems. Two-dimensional micro-mirrors have been studied for various applications (e.g, optical switches [1, 2], projection displays [3], and confocal microscopes [4]). Here we describe a MEMS-based beam steering actuator design and illustrate its potential application in a networked context.

The parameters that affect mirror performance are flatness, roughness, and reflectivity. Beam steering requires switching capabilities, and thus speed, maximum tilt angle, and power consumption are primary requirements. The design requires a tilt angle of +/- 5° and minimum power usage.

Some micro-mirrors have been fabricated with poly-silicon (poly) as the mirror material [5], which has limited deposition thickness and can affect dynamic performance at high resonant frequencies [4]. In this project, the mirror material is aluminum (Al) for high reflectivity. Also, to reduce manufacturing cost, the mirror material, beam, and springs are made of the same material and can all be at the same potential. The material used on the Al top electrodes is amorphous-silicon (a-Si) since it can be deposited at temperatures below 570° C. Due to the differences in thermal coefficient of expansion between a-Si and Al, induced stresses will cause deflection. However, voltages required for mirror tilt are independent of temperature since all four actuators (top electrodes) will deflect the same distance. Electrostatic actuation was provided using zipper actuators, which can provide large deflections using low voltages.

Section II covers the operating principles and the design considerations for the electrostatic actuator. Section III presents the simulation results of electrostatic actuation. Section IV introduces a thermal means of actuation to provide a 5° mirror tilt. Section V gives an outline of the field of networked control systems and application of the actuators therein. Section VI provides suggestions for additional investigation for minimization of voltage for electrostatic and of current for thermal actuation.

II. OPERATIONAL PRINCIPLES AND DESIGN CONSIDERATIONS

Figure 1 shows the schematic layout of the top plate actuator and the mirror, both of the same aluminum material, which simplifies the fabrication process. An added layer on the top layer of the cantilever beam is a-Si.

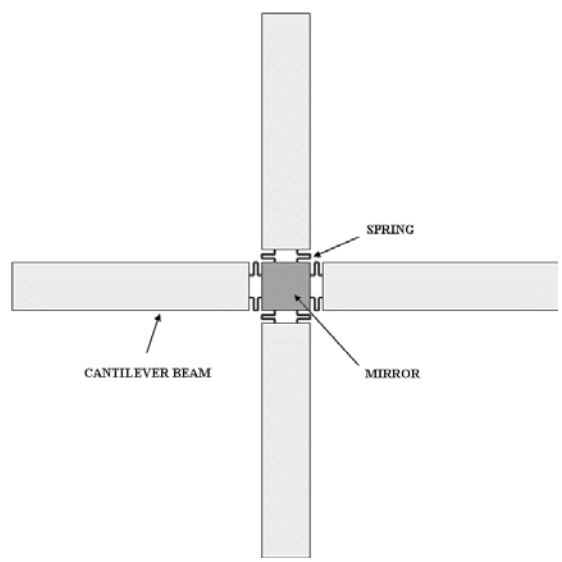

Figure 1. *Layout of mirror and top plates of the zipper actuator (Top View). The springs used provide stress relief for the mirror. The cantilever beam serves as the top electrode of the actuator. (Not to scale)*

Figure 2 shows the side view of the mirror, top and bottom plates of the actuator, spring, nitride, and air gap before release. The top plate and the mirror thickness (t) are the same in this design for ease of manufacturability. The top plate and the mirror are all at ground potential, while the bottom electrodes are used for positive potential. The length and width of the mirror are denoted as $L2$ with g as the capacitor gap.

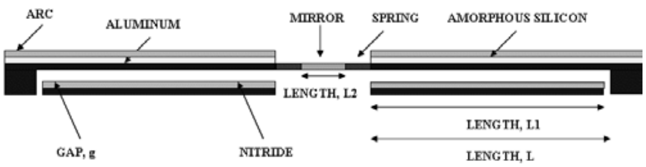

Figure 2. *A schematic view of the 2D beam steering structure before release. Note that an anti-reflective layer is used on top of the a-Si to ensure that the reflection is provided only by the mirror. (Not to scale)*

Note that there is no dedicated support for the mirror. The support is provided by the top plate and the springs of the actuator.

To model the top plate of the actuator, it was treated as a cantilever beam of length L, width W, and height or thickness, H (which is the same as t, the mirror thickness). An a-Si layer is on top of the top electrode to provide for aluminum expansion. An additional layer of anti-reflective coating (ARC) is present on top of the a-Si to ensure that the reflection of the beam is only supported by the mirror.

Zipper Actuator Process

The surface-micromachined cantilever beams of the zipper actuator consist of the following seven layers:

1) Nitride – This is the first layer of the process. It is deposited onto a silicon wafer to insulate the actuators from the silicon substrate, and also to provide a low-stiction surface for the filament.
2) Aluminum – This layer is used to form the contacts for actuation and beam support. The mask is used to selectively etch aluminum.
3) Nitride – This layer functions as a landing surface to prevent the top and bottom electrodes from being short-circuited. The nitride is etched away except at the bottom electrodes.
4) Oxide – Oxide is deposited 1 µm thick. This defines the air gap since it will be etched away using HF acid, allowing the beams to bend.
5) Aluminum - This layer is used to form the beam for the top electrode, the springs, and the mirror. Photolithography and etching define the structure.
6) Amorphous-Silicon – Amorphous silicon provides the stress needed due to different temperature coefficients of expansion compared to aluminum. These differences will provide the compressive and tensile stresses and consequently bend all the beams equally. The film need not be doped since aluminum is a conductor.
7) Anti-reflective – AR coating is finally used as the last layer to prevent unwanted reflections other than that provided by the 100 µm x 100 µm mirror. AR coating is used on all the beams.

After the structure is released, all the cantilever beams will be elevated to the same height and will lift the mirror, due to different temperature coefficients of expansion between Al and a-Si. The air gap is the primary factor that influences the forces on the cantilever beam due to applied voltages.

Design of the Zipper Actuator

Equilibrium condition states that the sum of forces in one direction should equal the sum of forces in the opposite direction. If the electrostatic force due to the actuator is F_e and the force from the cantilever beam due to deflection is F_b, then equation 1 results.

$$F_e = F_b \tag{1}$$

For simplicity, F_e can be modeled as a parallel plate capacitor given by

$$F_e = \frac{\varepsilon_r A V^2}{2g^2} \tag{2}$$

where ε_r is the dielectric permittivity for nitride (7.5 x 8.85 x 10^{-14} F/cm), A is the area of the capacitor (W x $L1$) cm^2, V is the applied voltage, and g is the gap between the top electrode and the bottom electrode. Width W is the width of the cantilever beam. Equation 2, however, would give error in calculating the voltage required for 5° tilt. The zipper actuator should be modeled as

$$F_e \sim E^{1/4} \frac{W}{\sqrt{x_{def}}} \left[\frac{\varepsilon_r V^2 H}{g} \right]^{3/4} \tag{3}$$

ε_r = Nitride dielectric permittivity = 7.5 ε_0
x_{def} = Cantilever deflection
V = Applied voltage
H = 0.5 µm (top electrode thickness)
g = 1 µm

$$E = \frac{\varepsilon_0 V^2 W}{2[g/\varepsilon_r]^2} = \text{Electric field}$$

Using the values above, voltages can be varied to determine the F_e required to cause a particular x_{def}. Equation 3 shows that F_e is dependent on $1/(x_{def})^{1/2}$ implying that changes in x_{def} due to temperature changes would not require much higher voltages for actuation.

The best part of the zipper actuator is that large deflections can be achieved with low voltages. The gap

(g) and the dielectric are the primary factors that influence the electrostatic forces. In order to build an efficient zipper actuator with low voltages, a value of 1 μm was chosen for g. The applied voltage V was varied to determine the mirror tilt angle. The length L and width W of the actuator were chosen to be 485 μm and 100 μm respectively.

The mechanical force due to cantilever beam is given by

$$F_{\mathrm{b}} = k_{\mathrm{c}} x_{\mathrm{def}} \tag{4}$$

where k_c is the spring constant of the cantilever beam and x_{def} is the deflection of the beam.

The spring constant of the cantilever beam is given by

$$k_c = \frac{E_{eq} W H^3}{4L^3} \tag{5}$$

where E_{eq}, W, H, and L are the Young's modulus for silicon or aluminum, width, thickness, and length of the cantilever beam respectively. The dimensions are given as

E_{Si} = 107 GPa
E_{Al} = 70 GPa
W = 100 μm (top and bottom electrodes)
L = 505 μm (cantilever beam length)
$L2$ = 100 μm (mirror length and width dimension)
$L1$ = 485 μm (bottom electrode length)
H = 2 μm (Al: 0.5 μm, Si: 1.5 μm)
E_{eq} = 94 GPa (simulation)

The difference in the mirror heights between the applied voltage electrode and the opposite electrode with no voltage will determine the angle. The difference required for 5° tilt is given by

$$\tan(\theta) = \frac{x}{L2} \tag{6}$$

with θ equal to 5° and $L2$ = 100 μm, x = 8.75 μm.

The springs also contribute to the overall mechanics as it does experience the forces due to electrostatic, cantilever beam, and the mirror mass, m. The spring structure used is given in Figure 3.

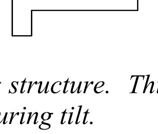

Figure 3. *The spring structure. This helps to reduce the stress on the mirror during tilt.*

The length, width, and thickness of the spring are 102 μm, 1 μm, and 0.5 μm respectively. The force due to the springs that also has to be overcome is given by

$$F_{\mathrm{s}} = k_{\mathrm{s}} x_{\mathrm{d}} \tag{7}$$

Note that x_{d} in equation 7 is the distance the springs will be pulled. The initial distance between the beam and the mirror is 8.75 μm. At 5° mirror tilt, the distance will be different due to the pull from the mirror and the cantilever beam.

The spring constants of the composite cantilever beam is 145.66 x 10^{-9} N/μm according to the simulation. For deflection of 8.75 μm, the mechanical force F_{b} due to the beam deflection is 1274.5 μN. This is the mechanical force that has to be overcome by the electrostatic force to give a 5° mirror tilt deflection. Using equation 3, it is determined that a voltage of approximately 63 V would be needed to give the desired mirror tilt angle. The equivalent mass of the composite beam is 0.91 x 10^{-10} kg, which is 13/35 of the static mass. The resonant frequency is about 4KHz.

The maximum bending stress occurs at the support and is given by

$$\sigma_{\max} = \frac{6L}{H^2 W} F_{\mathrm{b}} \tag{8}$$

Using equation 8, the maximum bending stress at the support is 152 MPa using F_{b} of 1.25 μN. This value will be compared to simulations in the next section.

III. ELECTROSTATIC SIMULATIONS

Simulations were performed using the dimensions specified in section II. The bottom part of the beam (Al) has more compressive stress than the top part of the beam (a-Si). Once the beam is released, the beam length increases slightly, relieving the compressive stress so that the average stress goes to zero. Once the beam is released, it bends, which produces a decrease in the tensile stress at the top of the beam and simultaneously a decrease in the compressive stress at the bottom of the beam. Figure 4 shows the simulated structure after release. This simulation was performed at room temperature (298 K) and the elevation was 25.3 μm for the mirror and 24.5 μm for the cantilever beams with zero applied voltages. Simulations and calculations show that a 5° mirror tilt can be obtained at 43 V with a similar mechanical force. The results shown in this project have a g of 1 μm.

The analysis included application of different voltages to determine the deflection and tilt angle θ. Figure 5 shows a non-linear relationship between θ and applied voltage.

Figure 4. *A simulated 2D mirror for beam steering after release. All four cantilever beams elevate and lift the mirror equal distances.*

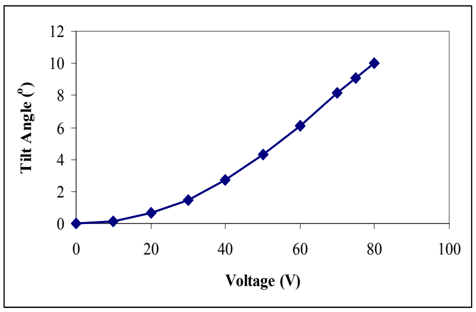

Figure 5. *Tilt Angle vs. Voltage applied. A non-linear relationship is displayed.*

The maximum stress at contact point D and mirror tilt of 5° is shown in Figure 6. One of the advantages of this technique is that the voltage required for mirror tilt is the same regardless of the outside temperature since the zipper actuator air gap is kept at a low 1 µm and that all the cantilever beams elevate to the same height. Stress at the contact from simulations was 130 MPa, quite close to calculated 152 MPa.

Figure 6. *A simulated 2D mirror for beam steering with maximum stress is at point D.*

To evaluate the rising (t_r) and settling (t_s) time of the actuator, the squeeze-film damping effects are considered dominant due to the gap between the substrate and the cantilever beam much smaller than its width.

$$Q \approx \frac{(E_{eq}\rho_{ave})^{\frac{1}{2}} WH^2}{vL^2}(\frac{g}{W})^3 = 2.9 \qquad (9)$$

where ρ_{ave} is the average density of the composite beam, 2440 Kg/m^3, and g is the gap between the substrate and the beam, with 13 µm as an estimation, H is the thickness of the composite beam, and V is the viscosity of 1.8 x 10^{-5} Nsm^{-2} (in air). Thus the damping coefficient is about 0.17. For the second order system, t_r and t_s are evaluated using

$$t_r = \frac{1}{\omega_d}\left(\pi - \arctan\frac{\sqrt{1-\xi^2}}{\xi}\right) \approx \frac{\pi}{2\omega_d} = 62.5\mu\sec$$
$$t_s \approx \frac{3}{\xi\omega_n} = 702\mu\sec \qquad (10)$$

If the device operates in the high vacuum, the Q will increase, the settling time will be much longer.

IV. THERMAL SIMULATIONS

An alternative approach to mirror tilt for beam steering is by thermal means. The overall structure remained the same with minor changes. Figure 7 shows the side view of the thermal actuator.

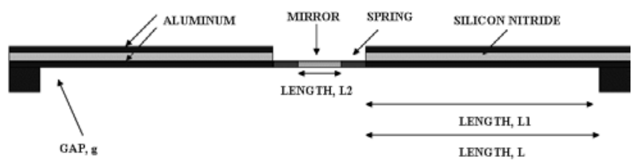

Figure 7. *A schematic view of the 2D beam steering structure before release for thermal actuation. (Not to scale)*

The mirror, springs, and cantilever beam including the top most layers (resistor) are all Al. The thermal energy is provided by using a snake/serpentine structure as resistor. The I^2R heating provides the thermal energy needed to cause beam deflection. The nitride is used because of its lower thermal conductivity compared to Al, which helps to minimize heat transfer to the mirror and springs and thus will minimize very small changes in the overall volume of the mirror. Also, nitride helps in the heat transfer from aluminum for cooling. In addition, since the thickness of the resistor is a low 0.1 µm, it will also maximize heat transfer from the resistor to air. The purpose of using Al at both ends is that it provides a mirror for high reflectivity and minimizes the stresses induced due to different temperature coefficients of expansion (as in electrostatic actuation where a-Si was used). The resistor layer on top of the nitride was much thinner than the main structure, which therefore has a much lower volume than the main structure and as a result would cause the beam to bend upwards. The main structure aluminum thickness is 0.5 µm and the nitride is 0.5 µm. The temperature was altered to simulate I^2R heating and the mirror tilt noted. The resistance of the aluminum resistor is given by

$$R = \rho L / A \qquad (11)$$

The length and area of the resistor is 3.64 x 10^3 µm and 1.5 μm^2 respectively. The resistance (R) is an increasing function of temperature since the resistivity (ρ) is an increasing function of temperature. The ρ for Al at 298 K and 400 K is 27.1 x 10^{-15} Ω-µm and 38.7 x 10^{-15} Ω-µm respectively. Using the values given above, the resistance at 298 K and 400 K is 66 pΩ and 94 pΩ respectively. Therefore, to actuate the beam at lower temperatures, the resistance can be increased by either reducing the overall length or increasing the area. As a result, lower currents I would be required to achieve the same deflections. Figure 8 shows the mirror tilt angle variation as function of temperature difference.

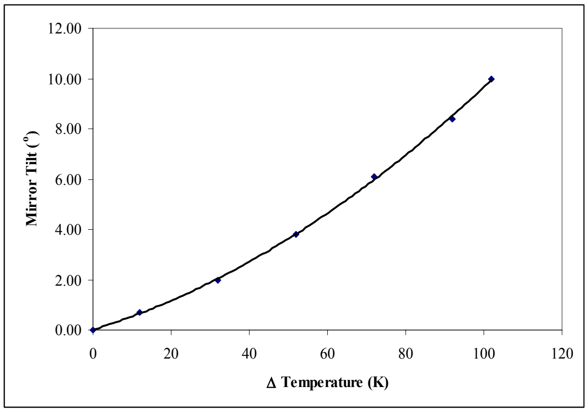

Figure 8. *Mirror deflection vs. ΔT. A non-linear relationship is displayed. The ΔT is the difference in temperature between the applied and room temperature of 298 K.*

The tilt is a non-linear function of temperature delta from room temperature of 298 K and can be written as

$$\theta = 0.0005(\Delta T)^2 + 0.0484(\Delta T) + 0.0104 \tag{12}$$

The heat flux J_Q through a bounding surface of a material is driven by temperature differences. The J_Q due to conduction is given by

$$J_Q = -\kappa \Delta T \tag{13}$$

where κ for aluminum and silicon nitride at 400 K is 2.4 x 10^8 W/K-m and 2.4 x 10^7 W/K-m respectively. Using the values for κ and ΔT of (400 – 298 K), the heat flux on aluminum resistor is 24 x 10^9 W/m. Simulations calculate the heat flux of each resistor strip at 4.9 x 10^9 W/m. The calculated heat flux has to be divided by five (a total of five spacings), which would equate to 4.8 x 10^9 W/m, very close to simulations. Heat flux on the nitride layer is simulated at 3.0 x 10^9 W/m and the calculated value is 2.4 x 10^9 W/m. The heat flux at the mirror is 1 x 10^{-4} W/m, a very low value indicating that the sandwiched nitride layer did help in eliminating heat transfer to the mirror and minimizing stresses or strains. Figure 9 shows a simulated linear relationship between the heat flux and the delta temperature as expected according to equation 13.

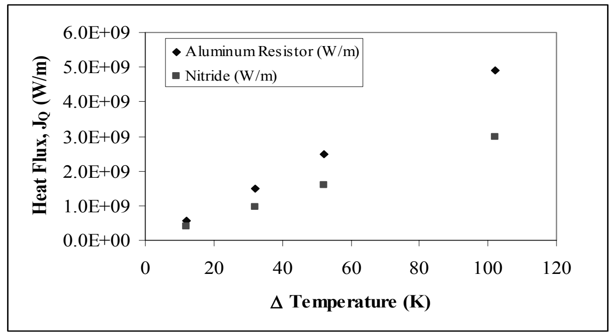

Figure 9. *Heat Flux vs. ΔT. A linear relationship is displayed. The ΔT is the difference in temperature between the applied and room temperature of 298 K.*

V. APPLICATIONS IN NETWORKED SYSTEMS

Technological and theoretical advances in areas such as communications networks and sensing have made it feasible to control systems across networks. Such a system is referred to as a networked control system (NCS) [6, 7]. This extension of the traditional hardwired control paradigm provides several advantages, including ease of configuration, fault tolerance, and component modularity. Therefore, there is significant motivation to provide both a developed theoretical underpinning for networked control systems and viable network-enabled devices.

Realizing the advantages of networked control systems comes with the price of managing the potentially performance-affecting and destabilizing timing effects of the communication network. Significant work has gone into the design of delay-tolerant control strategies and delay compensation schemes [8] and the theoretical exploration of the network medium [9]. Optimal control methods for linear systems have been established, and results have been derived to give bounds on the sensor sampling intervals that ensure system stability.

The development of networked control systems is also seeing the rise of new design paradigms, such as co-simulation for co-design [10], which asserts that the design of the communication network and the networked devices are critically intertwined. Thus, network-related issues (e.g., bandwidth) must be considered along with control-related issues (e.g., performance). The continuing progress of such techniques is crucial to the successful design of sophisticated networked devices.

In a MEMS context, networked control systems enable the construction of a device that operates at a distance from its control architecture. As such, the device can use lower power, even if subjected to more complex control strategies. More complex control strategies can be achieved by leveraging remote computational power, circumventing the limits of that which could be integrated into the MEMS device. Thus, the beam steering device could serve as the actuation component for an NCS testbed. One proposed architecture for such a testbed involves a mobile agent performing laser target tracking. In this case, the control communication is performed across a wireless network, allowing for the agent, controller, and separate scout sensing agents to be spatially distributed. This provides developed NCS-based functionality while allowing the study of complex issues involving the delays between sensors, controller, and actuators. In general, MEMS devices are prime candidates for networked devices since both size and power consumption are critical design factors.

VI. SUGGESTIONS FOR FUTURE STUDY

The stresses encountered, which were high during electrostatic simulations, can be reduced by investigating the following parameters:

1) Additional springs
2) Increased length of the cantilever beam

The voltage required for actuation can be reduced by:

1) Increased capacitor area
2) Increased length of the cantilever beam
3) Reduced dielectric gap

The current for thermal actuation can be reduced by:

1) Increased length of the resistor
2) Reduced area of the resistor

VII. CONCLUSION

An electrostatic and thermal actuation method was investigated for 2D beam steering. The electrostatic actuation was performed using a zipper actuator. The advantages of this design are the temperature insensitivity, process insensitivity, and low voltage for actuation. The model matched well with simulations, within a 5% error margin. An 80 V actuation was needed to provide a 5° mirror tilt. This voltage can be minimized to 60 V by reducing the dielectric gap from 1 μm to 0.25 μm. A non-linear relationship was found between the actuation voltage and mirror tilt angle. The natural frequency of the system was 74 kHz which was quite high for this system due to the low mass of the mirror and the low spring constants of the cantilever beam and springs. Additional force can also be provided by increasing the capacitor area which would then require even lower voltages. The mechanical force due to beam bending was approximately 2 μN which is quite low in spite of large deflections.

Thermal simulations showed a non-linear relationship between the temperature and the mirror tilt angle. A 400 K temperature was needed to achieve 5° mirror tilt. These temperatures can be reduced further by investigating the effects of length and area of the resistor. To minimize the effect of heat on the mirror, a 0.5 μm sandwiched nitride layer was utilized. Simulations showed that there was almost zero heat flux on the mirror compared to a high 4.9 x 10^9 W/m on the resistor strips.

The concept of networked control systems was reviewed, along with the potential applications for MEMS devices such as the beam steering device in the field. A summary of the issues and techniques in the field was also given. Particular advantages of the pairing such as reduced power consumption and increased control complexity were predicted.

ACKNOWLEDGEMENT

Thanks to Dr. Michael Branicky for his guidance in the networked control systems field and his input on its particular issues and properties.

This work was in part supported under National Science Foundation grant CCR-0329910.

REFERENCES

[1] P. M. Hagelin, U. Krishnamoorthy, C. M. Arft, J. P. Heritage, and O. Solgaard, "Scalable fiber optic switch using micromachined mirrors," *Proc. of 1999 Int. Conf. on Solid-State Sensors and Actuators*, Sendai, Japan, June, 1999.

[2] Z. Hao, R. Clark, J. Hammer, M. Whitley, and B. Wingfield, "Modeling air-damping effect in a bulk micromachined 2D tilt mirror," *Sensors and Actuators A: Physical*, 102(1-2):42-48, December 2002.

[3] H. Schenk, P. Durr, D. Kunze, H. Lakner, and H. Kuck, "A resonantly excited 2D-micro-scanning-mirror with large deflection," *Sensor and Actuators A: Physical*, 89(1-2):104-111, March 2001.

[4] H. Urey, D. W. Wine, and J. R. Lewis, "Scanner design and resolution tradeoffs for miniature scanning displays," *Flat Panel Displays, Proc. SPIE*, San Jose, CA, USA, January 1999.

[5] H. Toshiyoshi, W. Piyawattanametha, C. T. Chan, and M. C. Wu, "Linearization of electrostatistically actuated surface micromachined 2-D optical scanner," Journal of Microelectromechanical Systems, 10(2):205-214, June 2001.

[6] W. Zhang, M. S. Branicky, and S. M. Phillips, "Stability of Networked Control Systems," *IEEE Control Systems Magazine*, 21(1):84-99, February 2001.

[7] V. Liberatore, M. S. Branicky, S. M. Phillips, and P. Arora, Networked Control Systems Repository, http://home.cwru.edu/ncs/.

[8] J. Nilsson, "Real-time control systems with delays," Ph.D. dissertation, Department of Automatic Control, Lund Institute of Technology, Lund, Sweden, 1998.

[9] M. S. Branicky, S. M. Phillips, and W. Zhang, "Scheduling and feedback co-design for networked control systems," *Proc. IEEE Conf. on Decision and Control*, Las Vegas, NV, USA, December 2002.

[10] M. S. Branicky, V. Liberatore, S. M. Phillips, "Networked control system co-simulation for co-design," *Proc. American Control Conf.* Denver, CO, USA, June, 2003.